TECHNICAL REVIEW

No. 4 — 1982

Contents

SOUND INTENSITY (Part II. Instrumentation & Applications)

by

S. Gade, M.Sc.

ABSTRACT

In Part I of this article (Technical Review No.3 – 1982) the theoretical concept of sound intensity was described, and the different principles of signal processing were outlined.

In part II this article is continued, where the practical aspects of instrumentation are examined such as the requirements that have to be fulfilled in the design of the intensity probe, and how the phase mismatch between the two microphone channels can be eliminated. The signal to noise ratio achievable in the use of the two microphone technique is considered, and the instrumentation required for this technique discussed.

Finally, typical applications of sound intensity in the fields of sound power measurement and source localization are also illustrated.

SOMMAIRE

Dans la première partie de cet article (Revue technique No.3-1982) nous avons vu le concept théorique de l'intensité acoustique, et notamment les différents principes de traitement du signal.

Dans la deuxième partie de cet article nous verrons les aspects pratiques des instruments, comme par exemple les exigences qui doivent être remplies par la Sonde d'intensité acoustique, et comment on peut éliminer le déphasage entre les deux voies microphoniques. Le rapport signal sur bruit obtenu avec la technique des deux microphones est considéré, et l'appareillage requis pour cette technique est discuté.

Finallement, des applications caractéristiques de l'intensité acoustique dans les domaines de la mesure de puissance acoustique et de la localisation des sources sont montrées.

ZUSAMMENFASSUNG

In Teil 1 dieses Artikels (Technical Review Nr. 3 – 1982) wurde die Theorie der Schallintensität und die verschiedenen Methoden zur Signalbehandlung beschrieben.

In Teil 2 werden die praktischen Aspekte der Instrumentierung untersucht, wie die Anforderungen, die an die Konstruktion der Mikrofonsonde gestellt werden müssen und wie sich Phasenfehlanpassungen der beiden Kanäle vermeiden lassen. Das mit der Zwei-Mikrofontechnik erreichbare Stör/Nutzsignalverhältnis und der notwendige Meßaufbau werden diskutiert.

Schließlich werden typische Anweudungsbeispiele der Schallintensitätsmessung zur Schalleistungsbestimmung und zur Schallquellenortung gegeben.

9. Eliminating Phase Mismatch

There exists a rather simple method to eliminate a possible phase mismatch between the two channels, simply by calculating the average intensity of the 2 measurements, where the second measurement is performed with the two microphone positions interchanged. The basic idea of the switching technique is to interchange those parts of the measuring chains where there is phase-mismatching. Those parts have to be interchanged at two points in the measuring chain.

Thus, to eliminate phase-mismatching of the full measuring chains, the microphone positions have to be interchanged (point 1) and the sign of the spectrum must be changed (for point 2). It is shown in Appendix G that this procedure leads to the approximation error formula

$$\frac{\hat{I}_r}{I_r} = \frac{\sin(k\Delta r)}{(k\Delta r)} \cos\varphi \qquad (9.1)$$

It is seen from equation 9.1 that the error due to a phase mismatch is independent of frequency and spacing, and in practice becomes negligible.

Note that in general a correction for phase mismatch is not necessary when using B & K Sound Intensity System, since matched components for the two channels and digital filter techniques are used.

On the other hand, when using unmatched microphones or tape recordings of the signals, correction for the phase mismatch is essential for sound intensity calculations. For dual channel FFT-analysis, there exist

several correction methods and the 3 most commonly used procedures will be discussed in the following. Mathematical treatment and further discussion of the 3 procedures is found in Appendix H.

For the TRANSFER FUNCTION METHOD the calibration of the microphones is accomplished by mounting both microphones on a plate that can be rigidly attached to the end of a duct. The two microphones are then assumed to be exposed to the same sound field. The transfer function K_{AB} between the two channels is then measured and used for correction of all subsequent measurements, since K_{AB} contains information of phase and amplitude differences between the two channels.

$$S_{p_1 p_2} = \frac{S_{AB}}{|H_A|^2 \cdot K_{AB}} \tag{9.2}$$

where $S_{p_1 p_2}$ is the cross-spectrum of the sound field
S_{AB} is the measured (FFT calculated) cross spectrum
and $|H_A|^2$ is the gain factor of channel A.

Calculation for this method is easy, but it is difficult to determine K_{AB} over a wide frequency range due to resonances of the duct system. Typically, this method is valid up to 4 kHz. Furthermore calibration must be periodically repeated on account of drift problems.

The advantages and disadvantages of interchanging the microphones during the measurement, also called the MICROPHONE SWITCHING METHOD are just the opposite of those of the transfer function approach.

$$S_{p_1 p_2} = \sqrt{\frac{S_{AB} \cdot (S'_{AB})^*}{|H_A|^2 \cdot |H_B|^2}} \tag{9.3}$$

Eqn.(9.3) shows that it is the geometrical mean of the two cross spectra that is used instead of the arithmetic mean. Calculation of the intensity by the use of this method is more complicated because complex multiplication and square root extraction is required. Besides the measurement time is increased by a factor of two. However, no further calibration is needed and the above mentioned frequency limitations are eliminated for this method.

A third method, the MODIFIED MICROPHONE SWITCHING METHOD is a compromise between the two methods described, utilizing the advan-

tages of both methods, so that broad band measurements are carried out in a shorter measurement time.

10. Dynamic Range and Signal to Noise Ratio

Normally signals representing sound pressure will be contaminated by noise, predominantly, from microphones or preamplifiers.

By use of the two microphone technique extremely low sound pressure levels can be measured, since uncorrelated noise in the two channels is cancelled. Consequently, the dynamic range of an intensity meter is larger than for the corresponding sound level meter. In practice this is only true for relatively high frequencies, due to the influence of the time integrator.

The spacing Δr between the microphones is a scaling factor, since the output of the intensity meter is proportional to the microphone spacing (equation 4.1). Hence a choice of a larger spacer improves the signal-to-noise ratio.

At low frequencies where the difference between two nearly equal pressure signals is used for the calculations of the particle velocity, the signal to noise ratio will be poor. In fact, it is seen from equation 4.2 (Technical Review No.3–1982) that the dynamic range is proportional to the frequency.

11. Probe Design

In the probe design there are several requirements which must be fulfilled. The ideal intensity probe should consist of 2 microphones with identical phase response and have a flat amplitude response as a function of frequency. Furthermore the presence of the probe should disturb the sound field as little as possible. The shadowing effect of one microphone on the other microphone should also be minimized for all frequencies of interest. Finally, the effective acoustical separation distance must be constant and frequency independent, since this distance is a scaling factor.

Possible microphone configurations take 3 main forms, which normally are termed "face to face" "side by side" and "back to back" (see Fig.16).

Investigations have shown that a "face to face" probe configuration with a solid spacer between the two microphone grids gives the best

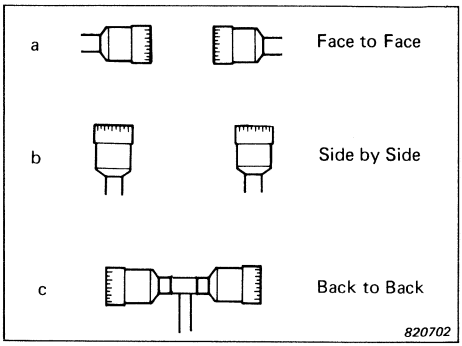

Fig. 16. Different probe configurations

performance and therefore is the best choice. (Ref. [21], [23], [29]).

This configuration (shown in Fig.17) produces between the cylindrical spacer and the diaphragm of each microphone a small volume which is acoustically coupled to the sound field via the slits in the microphone grid. Thus the incident sound field activates the diaphragm only via the peripheral slits.

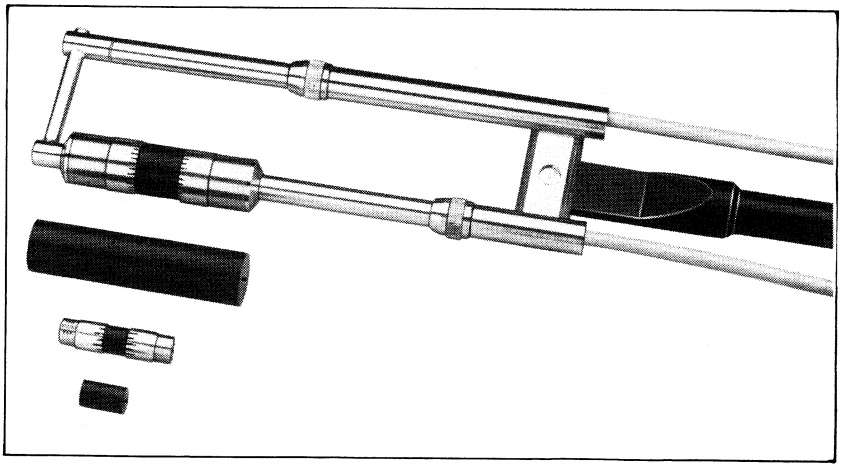

Fig. 17. Sound Intensity Probe Type 3519 showing the two 1/2'' microphones separated by the 12 mm spacer. The 1/4'' microphones are separated by the 6 mm spacer

A small change in sensitivity of the microphones with and without the spacer in front of the grid has been taking into account, when adjusting the B & K Sound Intensity Analyzer, for intensity measurements.

The amplitude response measurement for the probe consisting of 2 free field corrected pressure microphones has been carried out using B & K FFT-Narrow Band Analyzer Type 2031. The distance between sound source and microphone probe was 1,5 m and plane progressive waves assumed in an anechoic chamber. The variation in amplitude response is shown for 0° incidence in Fig.18. The two upper curves show the response for the 2 microphones as they are mounted in the probe. These curves show a nearly flat frequency response for both microphones which of course is desirable but on the other hand not essential. The lower curve shows the difference between these two curves and leads directly to a part of the shadow effect error from the probe. $p_B - p_A$ is less than 0,5 dB for all frequencies of interest.

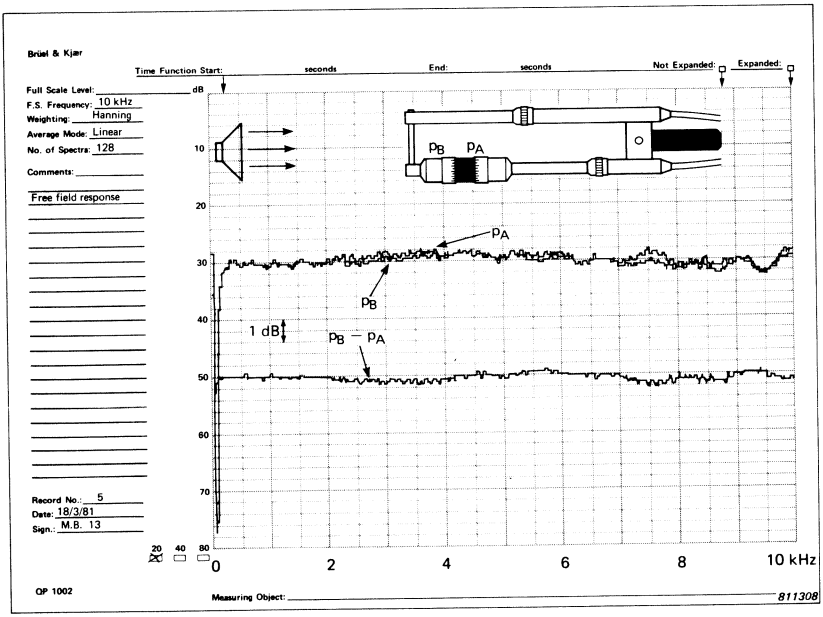

Fig. 18. Free field responses. The pressure at the two microphones, denoted by p_A and p_B, was measured with the probe aligned along the direction of sound propagation and the difference $p_B - p_A$ determined

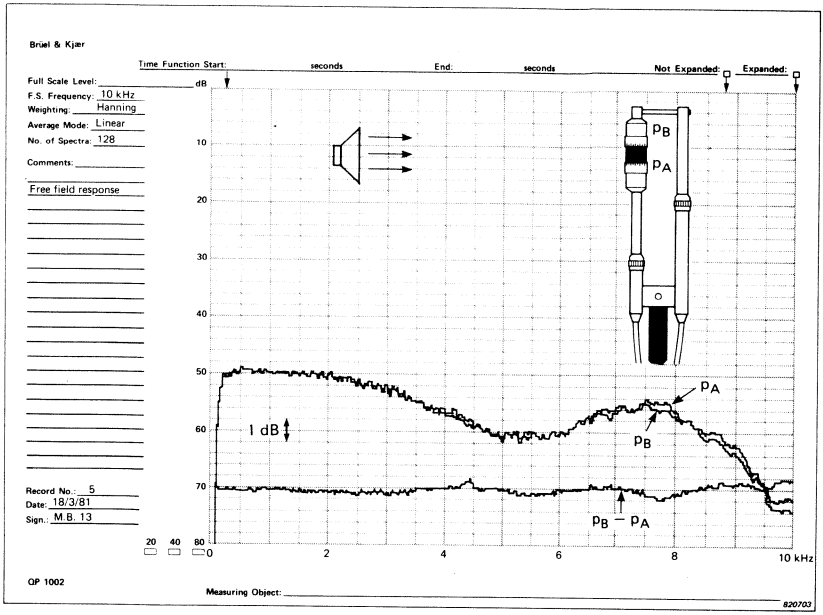

Fig. 19. Free field responses. The pressure at the microphones measured with the probe aligned perpendicular to the direction of sound propagation

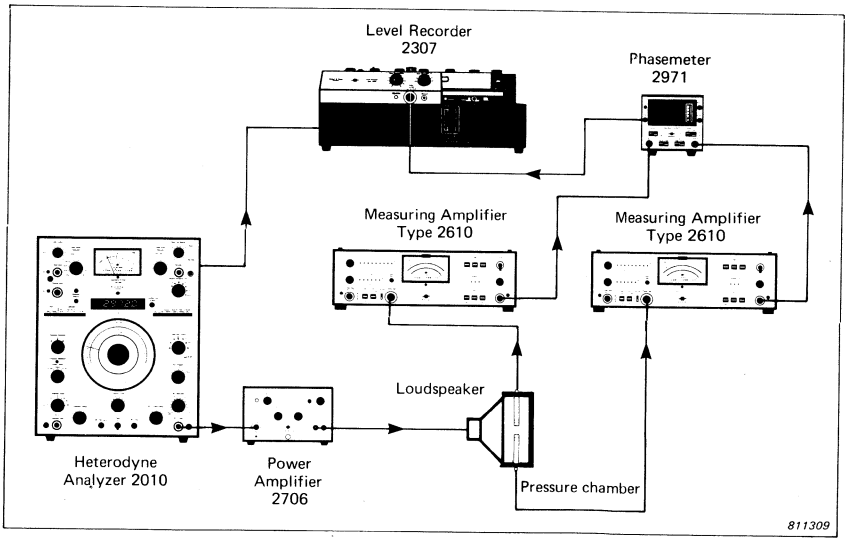

Fig. 20. Set-up for measurement of phase mismatch

As another example, sound incidence of 90° is used, and Fig.19 shows the reflection from one of the preamplifiers around 7,5 kHz, though it should be noted that the most important curve $p_B - p_A$ is still rather independent of frequency.

The microphones supplied with the probe are paired on the basis of results of phase-matching measurements in a pressure chamber (see Fig.20). A typical calibration chart for Condenser Microphone Cartridge Pair Type 4177 is shown in Fig.21. Note that the two curves are from two relative measurements, the second measurement performed with the two microphones interchanged. This procedure improves the resolution of the calibration by a factor of 2. Also any influence due to a possible cartridge capacitance deviation will be suppressed by this calibration method.

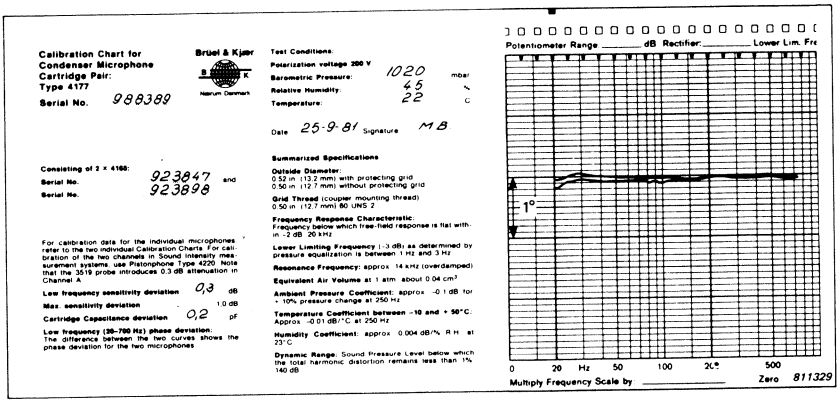

Fig. 21. Typical calibration chart for Condenser Microphone Cartridge pair 4177

Since the microphone separation is a scaling factor, it is very important that the effective acoustical separation between the microphones is as frequency independent as possible. Here again the face to face (slit grid) configuration shows the best performance especially above 2 – 3 kHz. The solid cylindrical spacer between the microphones forces the sound field to be sampled through the slits of the protection grid, and hence also "forces" the acoustic distance to be rather well defined. In fact variations in the effective separation express the disturbance of the phase curves of the microphones due to diffraction and scattering phenomena. The measurement set-up is shown in Fig.22. Fig.23 shows the variation of the effective microphone separation about the nominal

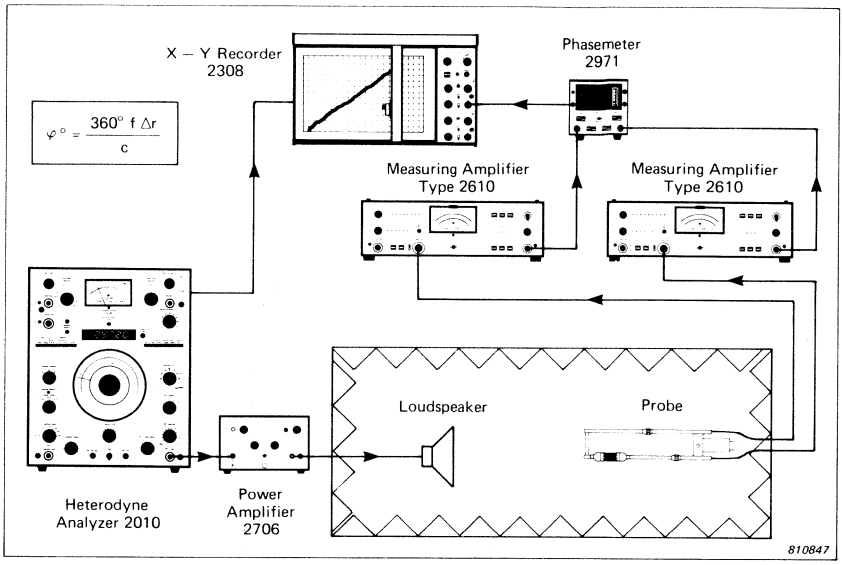

Fig. 22. Set-up for measurement of effective microphone separation

value of 12 mm as a function of frequency for the 2 most commonly used configurations – the side by side and face to face.

Apart from fulfilling the obvious specifications, the design of the intensity probe should facilitate quick calibration (microphones should

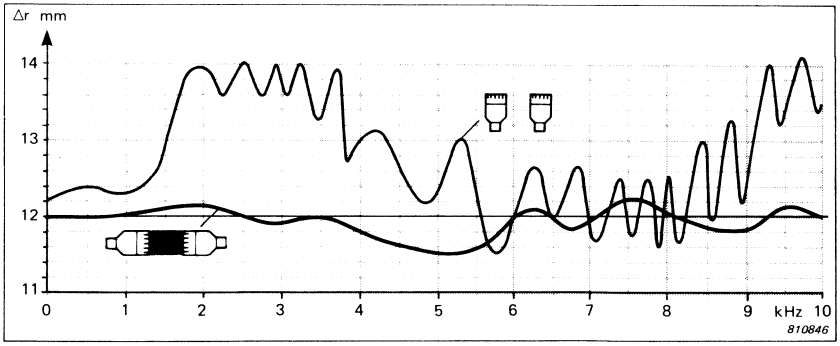

Fig. 23. The variation of the effective microphone separation about the nominal value of 12 mm as a function of frequency

be readily separable for use with pistonphone). Furthermore, it should be relatively easy to change the microphones between 1/2'' to 1/4'' and the microphone separation distances. All these facilities have been taken into consideration in the construction of the probe shown in Fig.17.

Fig.24 shows the frequency range for the various microphones and spacer configurations for a measurement accuracy of ± 1 dB. The number of 1/3 octave bandwidths is given by

$$BW(\pm 1dB) \approx 3\, log_2(1/4\varphi) \approx 16 \qquad (11.1)$$

As can be seen, the useful frequency range depends only on the degree of phase matching φ independent of the microphone spacing.

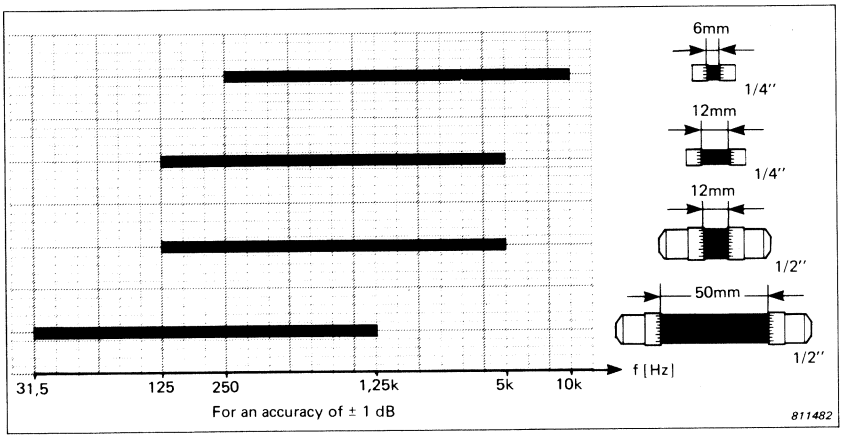

Fig. 24. Frequency range for the various microphone and spacer configuration for a measurement accuracy of ± 1 dB

12. Instrumentation Techniques

Three different types of instrumentation exist today for intensity calculations, all based upon the use of two closely spaced microphones:

1. Using small transportable analogue based instruments, where the intensity is measured over broad band (e.g. linear, A-weighted) or in octaves.

If only the overall level is needed, or when working on large machines which are difficult to move about, a small analogue meter might be the best choice – and the cheapest.

Today, the problem of matching analogue filters has largely been overcome, but normally the calculation can only be carried out in one band at a time.

2. Dual channel FFT-analysis, where the intensity is calculated from the imaginary part of the cross-spectrum function, can be used where there is a need for very narrow band resolution and where the blockwise analysis is no limitation (e.g. for analysis of stationary signals).

3. By using digital filter techniques, which permit evaluation of the intensity by the use of a double digital filterbank operating in real time with normalized 1/3 octave and 1/1 octave filters. (see Fig.25). The Brüel & Kjær Sound Intensity Analyzer Type 2134 is based upon this principle.

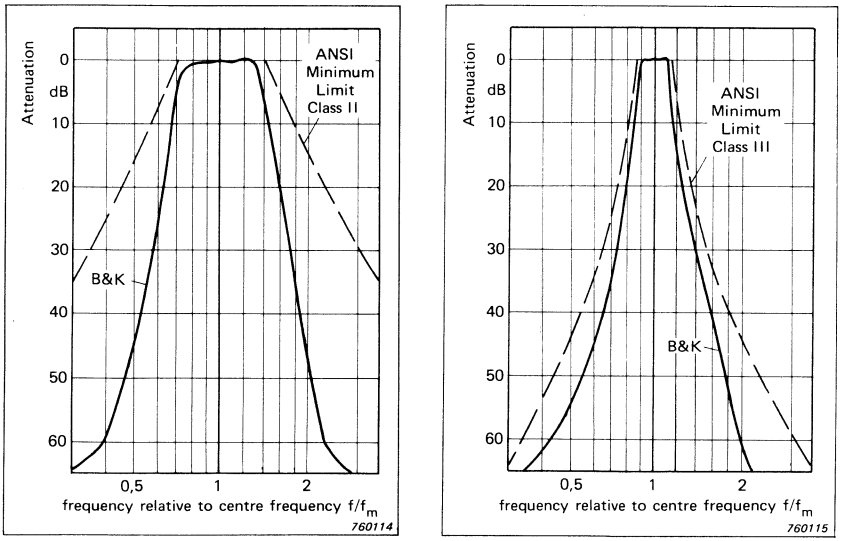

Fig. 25. Octave and 1/3 octave filter characteristics of the 2134 Intensity Analyzer

For fluctuating signals (often encountered in acoustics) and where speed is of importance the real time digital filter analyzer is the best choice.

Digital filter techniques are described in Ref.[14], [15], [16], [17] and [30]. The design of the digital time integrator is discussed in Appendix I.

13. Applications

13.1. Sound Power Determination

One of the principal applications of sound intensity measurements is the determination of sound power radiated by sound sources. In fact, the radiated sound power can be determined from intensity measurements on a suitable surface enclosing the source, since the intensity describes the power passing through an area.

$$W = \int\int_S \vec{I} \cdot d\vec{A} = \int\int_S I_n \cdot dA \qquad (13.1)$$

The integration (or in practice the summation) over the above-mentioned enclosing surface of the intensity component normal to the surface, I_n, will directly give the power of the source, L_W (see Fig.26).

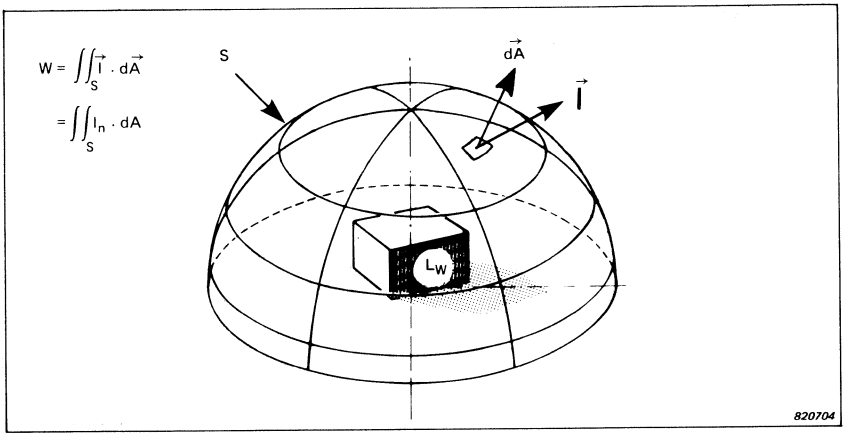

Fig. 26. Calculation of sound power from Sound Intensity Measurements

Some of the advantages of using intensity rather than sound pressure measurements for determining sound power are:

1. There are no restrictions upon the sound field which implies that the measurements can be performed in any room. On the other hand, the sound power emitted by a source may depend on the impedance of the environment.

2. Measurements can be carried out in the near field as well as in the far field. Nearfield measurements improve the signal to noise ratio and require less space, but the number of measurement points may have to be increased.

3. There are no restrictions upon the enclosing surface. Any shape can be used.

4. The method excludes any influence from contaminating sound fields.

In the case where a sound source is placed outside the enclosing surface the net flow through the surface from this source is zero (Gauss' theorem). Thus the background noise will be eliminated from the sound power measurement, which means that the sound power of individual parts of large machines can be measured by the use of the intensity method (Fig.27).

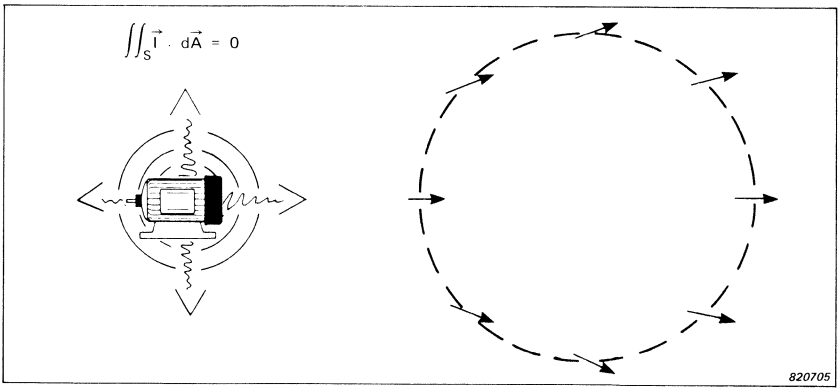

Fig. 27. Acoustic source not situated within the enclosing surface. This is Gauss' Theorem and is valid provided there is no absorption within the enclosing surface

This is of great importance when measurements are performed on, for example, gearboxes or pumps, which normally must be driven by motors and loaded as under normal conditions to obtain realistic results, Ref.[31].

As an example, measurements were performed on a motor and a pump coupled together (see Fig.28). The total radiated Sound Power from the system was 87,7 dB(A), while the Sound Power from the unloaded motor was 65 dB(A). In this case there was no doubt that the pump was the cause of the high level noise.

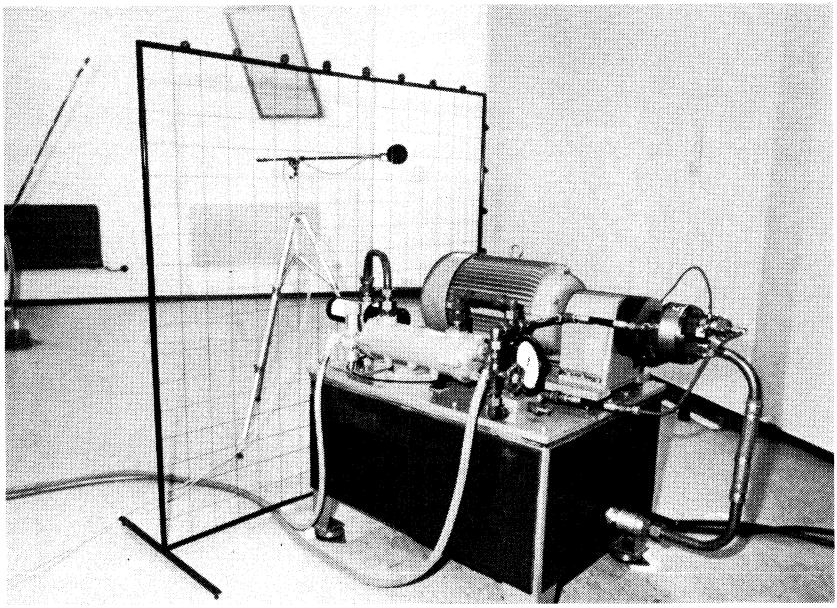

Fig. 28. Sound Power Measurements of a motor and a pump coupled together. Note the grid which is used for easy determination of the measurement points

On the other hand, intensity measurements revealed that the radiated Sound Power was 85,8 dB(A) from the motor and 83,2 dB(A) from the pump, when the two units were coupled together. The explanation is that the motor acts as a loudspeaker for the pump via the coupling. (Ref.[26]).

Another application example is discussed in Ref. [25]. In this case measurements were performed on a large labelling machine in the tapping hall of a brewery, where a high level of background noise was present.

It should be noted that sound power determination, wherever possible, should be carried out using sound pressure measurements. This is because:

1. In general intensity method requires more measurement points than the corresponding sound pressure method, because of the added complexity of the intensity sound field. In practice this is a minor problem when using a real time analysing system.

2. Today (late 1982) there exist no national or international standards for intensity method of sound power determination.

3. The use of different spacers for the intensity probe is required to cover more than 5 octave bands within an accuracy of $\pm$ 1 dB.

13.2. Noise Source Location

The second main application of sound intensity measurements is noise source location, or detection of "acoustic leaks" in structures. Several methods can be used:

1. Comparison Method

One method is to sweep the probe in 0° positions, i.e. perpendicular to the surface, back and forth close to the surface whilst watching the display screen.

When an area with high intensity level is discovered, the spectrum can be stored and the investigation continued. A further spectrum is stored and compared with the previous one. In this manner the most serious offender can be singled out for further investigation.

2. Continuous Sweep Method

A second method, the "continuous sweep" method, utilises the sharp minimum in the directional characteristics of the probe, (the probe in 90° position, i.e. parallel to the surface), see Fig.5 in Technical Review No.3 – 1982.

A passage of the source through the minimum in any octave or 1/3 octave band is indicated on the Display Unit Type 4715 by a rapid change in the brightness of the corresponding bar on the display screen showing a change from "positive" to "negative" intensity and vice versa (see Figs.29 and 30).

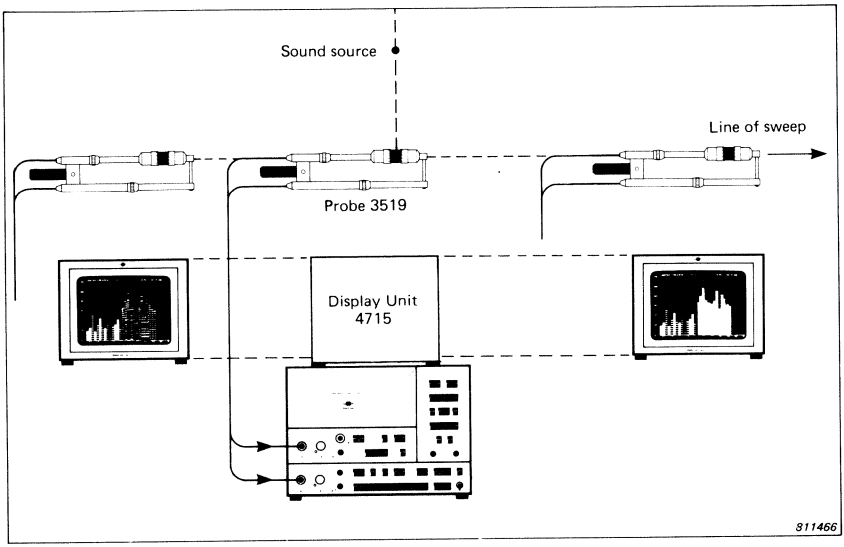

Fig. 29. Continuous sweep method for locating sources. As the median plane of the probe is swept past the source, the intensity spectrum shown on the display changes in brightness, indicating that the intensity is now incident from the rear hemisphere of the probe and not the front hemisphere

3. Intensity Mapping

For intensity mapping the area of interest is broken down into a grid, and the normal component of the intensity vector is measured at each point on the grid (Fig.28). The spectra obtained are then entered into a computer or calculator (for field measurements into the Digital Cassette Recorder Type 7400, see Fig.31) which through the use of an interpolation method converts the data into maps of intensity across the entire grid for each frequency band of interest. Various methods can be used to represent these maps; one is to plot equal-intensity contours, another is to use 3-dimensional contours. An equal-intensity contour map is shown in Fig.32, which shows the variation in intensity close to the surface of the engine cover of a van (Ref. [19]).

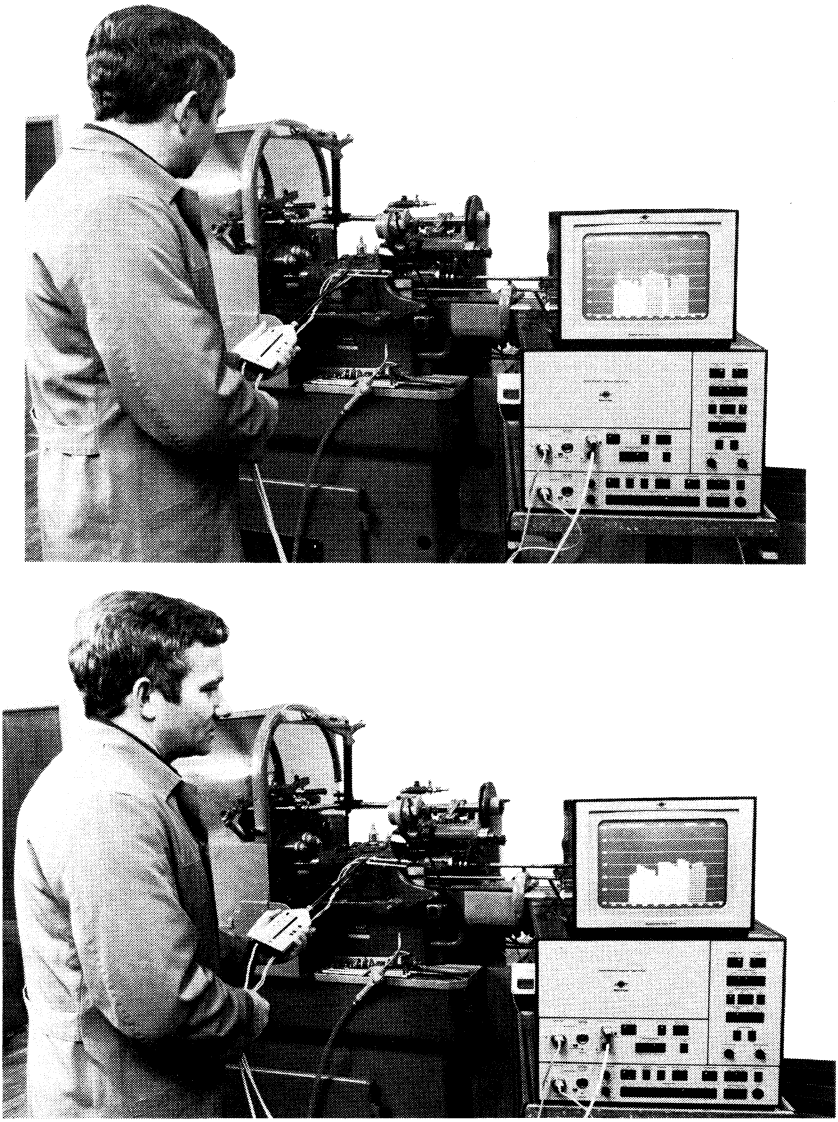

Fig. 30. Continuous sweep method for locating sound sources on a small lathe. As the median plane of the probe is swept past the source, i.e. the pulley and gear housing, the mid-frequencies of the displayed intensity spectrum change in brightness

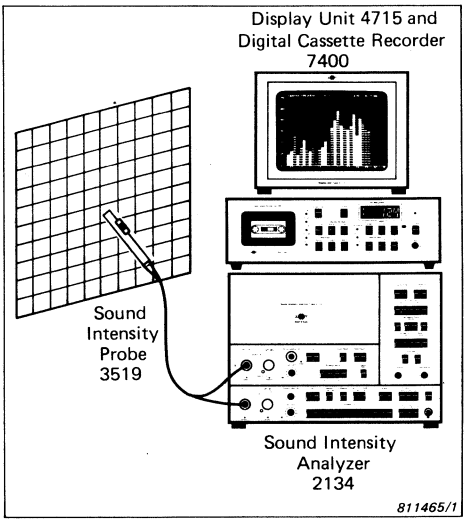

Fig. 31. Data storage on Digital Cassette Recorder Type 7400. One cassette contains more than 1200 third octave spectra or 2400 octave spectra

To make it easier to distinguish between "positive" and "negative" intensity contours different colours are used. The red colour indicates "positive" intensity and the blue colour "negative" intensity.

The same data are presented in 3-D plots in Fig.33 and Fig.34; "positive" and "negative" intensities are shown separately in 2 plots.

The term "positive" intensity is used where a net flow of acoustic energy is emitted from the surface of a machine, in which case work is done upon the air. Such a surface is often called a sound source.

A sound sink is defined as the surface where "negative" intensity is located. In this case it is the air which does work upon the surface, since "negative" intensity indicates a net flow of acoustic energy towards the surface. As shown in Fig.32, Ref.[19] it is quite possible to find sources and sinks beside each other on the same machine.

The reason might be that for very close measurements, e.g. only a fraction of a wavelength, from the surface of a vibrator, not all the waves would be propagating waves. Some are evanescent waves, whose amplitudes decrease exponentially with distance from the

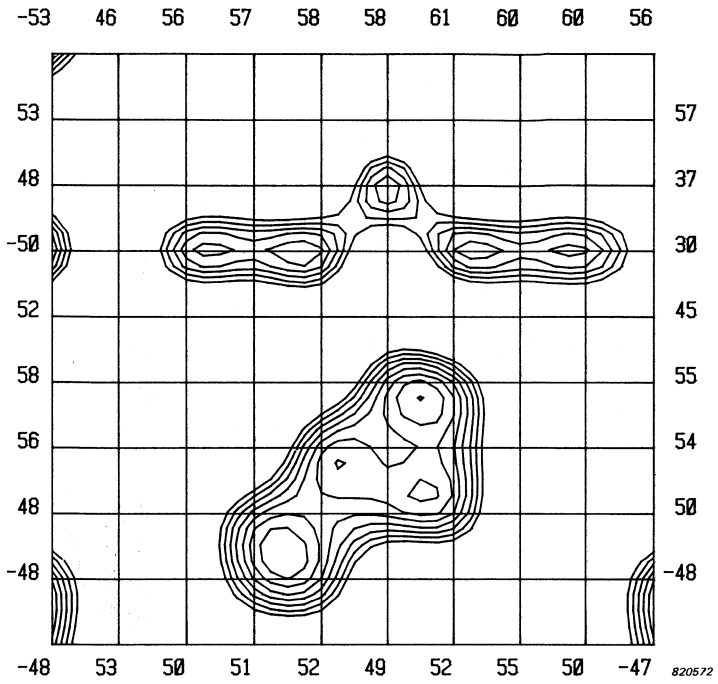

Fig. 32. Equal intensity contour map measured with 12 mm spacer over the engine cover of a VW-van at 315 Hz

source. In highly reactive sound fields, e.g. close to a vibrator, also circulating energy flow would be found, that is, energy which may leave a part of the vibrating surface only to turn around quickly, within a wavelength, and flow back into another part of the surface. The energy is then returned through the vibrator back to the "source" area. (Ref. [20, 32]).

This clearly demonstrates that sometimes maps of intensity must be interpreted with caution. In general the spatial resolution must be *smaller* than the wavelength of sound, but to avoid influence of the evanescent waves, below the coincidence frequency, the spatial resolution must also be *larger* than the wavelength of the vibrator. Furthermore, one must perform a space-time-averaging, by letting the probe sweep back and forth over the surface element during the measurement time, instead of performing point measurements (Ref.[18]).

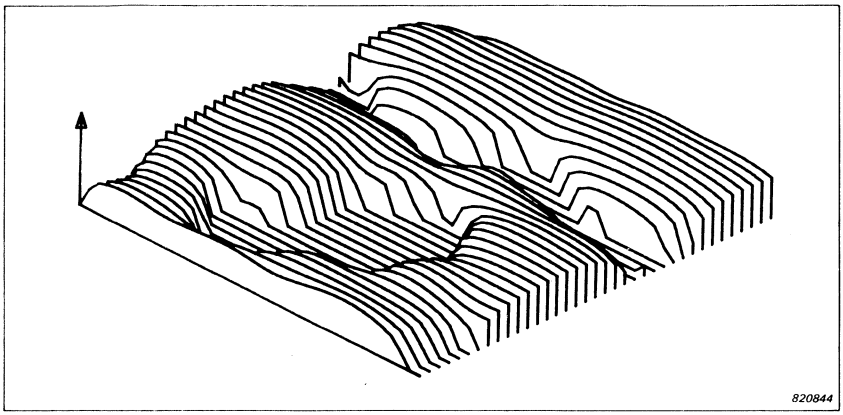

Fig. 33. 3-D plot of normal intensity over the engine cover at 315 Hz. Only "positive" intensity, that is where the acoustic sources are located, is shown

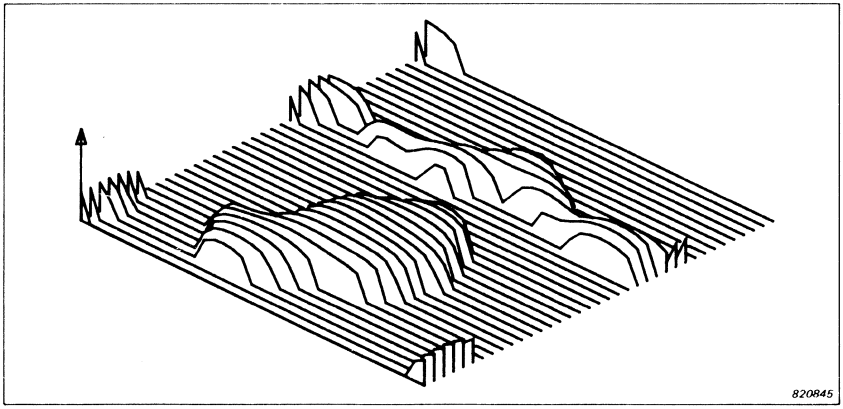

Fig. 34. 3-D plot of normal intensity over the engine cover at 315 Hz. Only "negative" intensity, that is where the acoustic sinks are located, is shown

13.3. Sound Absorption

In-situ measurements of sound absorption coefficients can be mentioned as a third application example. The absorption coefficient is defined as the ratio between the absorbed sound energy to the incident sound energy. The absorbed energy can be determined from the

average value of the intensity distribution over the absorbing surface. The incident energy can be estimated from sound pressure measurements in the room (Ref. [21]). For example in a reverberant room equation 2.3 (Technical Review No.3.–1982) can be used for estimating the incident energy.

13.4. Sound Reduction Index

As a last application, it can be mentioned that transmission loss (Sound Reduction Index) measurements can be performed with the use of only one reverberation room instead of a transmission suite (Ref. [27]).

14. Conclusion

To summarize, the B & K 2 channel Real Time Sound Intensity Analyzing System Type 3360 based upon digital filtering techniques opens new horizons for acoustical measurements. The instrument operates both in sound pressure mode (from 1,6 Hz to 20 kHz third octave centre frequencies) and sound intensity mode (from 3,2 Hz to 10 kHz third octave centre frequencies).

For many applications there is a distinct advantage in measuring the vector quantity, sound intensity, rather than the scalar quantity, sound pressure.

Traditional sound pressure measurements register noise levels at the receiver (the effect), but only sound intensity measurements are able to reveal where the sound is coming from (the cause).

References

[14] ROTH, O.: "Digital Filters in Acoustic Analysis" *B & K Technical Review* No. 1–1977 – part 1.

[15] UPTON, R.: "An Objective Comparison of Analog and Digital Methods of Real-Time Frequency Analysis." Brüel & Kjær, *Technical Review* No.1.–1977.

[16] RANDALL, R.B.: "Frequency Analysis". *Brüel & Kjær 1977.* pp-160–184.

[17] FAHY, F.J. & ELLIOT, S.J.: "Practical Considerations in the choice of transducers and signal processing techniques for sound intensity measurements." *Acoustic Intensity – Senlis* 1981, pp. 37–44.

[18] CHUNG, J.Y.: "Fundamental Aspects of the Cross-spectral Method of Measuring Acoustic Intensity." *Senlis* 1981, pp. 1–10.

[19] GINN, K.B. & GADE, S.: "Sound Intensity Measurements inside a motor vehicle." *B & K Application Note,* 1982.

[20] MAYNARD, J.D. & WILLIAMS, E.G.: "A New Technique for Noise Radiation Measurement." *Noise-Con.* 1981, pp. 19–24.

[21] FAHY, F.J.: "Practical Aspects of Sound Intensity Measurement." *Institute of Acoustics,* Spring Conference 1982, pp. B.1.3.1 – B.1.3.4.

[22] BENDAT, J.S.: "Acoustic Intensity Measurements." *Notes* 1982.

[23] FREDERIKSEN, B.W.: "Sound Intensity Measurements of Machinery Noise". *Brüel & Kjær 1980.*

[24] HEE, J., GADE, S., GINN, K.B. & CORNU, P.: "Sound Intensity Measurements inside aircraft". *B & K Application Note 1982.*

[25] GADE, S, WULFF, H., & GINN, K.B.: "Sound power determination using sound intensity measurements, Part I". *B & K Application Note 1982.*

[26] GADE, S., THRANE, N. & GINN, K.B.: "Sound power determination using sound intensity measurements, Part II". *B & K Application Note 1982.*

[27] CROCKER, M.J., FORSSEN, B., RAJU, P.K. & WANG, Y.S.: "Application of Acoustic Intensity Measurements for the Evaluation of Transmission Loss of Structures." *Senlis 1981,* pp. 161–169

[28] ROTH, O., GINN, K.B. &, GADE, S.: "Comparison of sound power determinations from sound pressures and from sound intensity measurements." *B & K Application Note 1982*

[29] RASMUSSEN, G., & BROCK, M.: "Acoustic Intensity Measurement Probe." *Acoustic Intensity – Senlis 1981,* pp.81-84.

[30] RANDALL, R.B. & UPTON, R.: "Digital Filters and FFT Technique." *B & K Technical Review,* No.1–1978.

[31] LAMBERT, J.M.: "The application of a Modern Intensity-Meter to Industrial Problems: Example of in-situ sound power determination", *Internoise 79*, pp.227-231.

[32] FRIUNDI, F.: "The utilization of the Intensity-Meter for the investigation of sound radiation of surfaces." *Unikeller* 1977

APPENDIX G

Phase Mismatch, Correction Procedure
Interchanging microphones

$$\hat{I}_{r,s} = \frac{1}{2}(\hat{I}_r - \hat{I}'_r)$$

$$= \frac{1}{2}(|\hat{I}_r| + |\hat{I}'_r|)$$

$$= \frac{1}{2} I_r \frac{\sin(k\Delta r - \varphi) + \sin(k\Delta r + \varphi)}{k\Delta r}$$

$$= I_r \frac{\sin(k\Delta r)}{k\Delta r} \cos\varphi \qquad \text{(G.1)}$$

where φ is the phase mismatch. The error is less than 0,1 dB for $\varphi = 12°$.

APPENDIX H

FFT-Corrections and Calibration Methods
The basic relation used for all calculations is

$$S_{AB} = S_{p_1 p_2} \cdot H_A^* \cdot H_B \qquad \text{(H.1)}$$

where S_{AB} is the "measured" cross-spectrum or the FFT-calculated cross-spectrum. $S_{p_1 p_2}$ is the cross-spectrum of the sound field at the position of the 2 microphones. This means that in eqn. D.13 (see Technical Review No.3–1982), the quantity S_{AB} should be written in full form $S_{p_1 p_2}$. H_A and H_B are the transfer functions of the two measuring channels.

H.1 Transfer Function Approach

If the same sound field is applied to the two microphones (e.g. by use of a duct as shown in Fig.H1) we obtain

$$S_{AB} = S_{pp} \cdot H_A^* \cdot H_B \tag{H.2}$$

The measured autospectrum from channel A is

$$S_{AA} = S_{pp} \cdot H_A^* \cdot H_A \tag{H.3}$$

Hence we have

$$K_{AB} = \frac{S_{AB}}{S_{AA}} = \frac{H_B}{H_A} \tag{H.4}$$

The ratio between the transfer functions of the 2 channels is simply obtained by taking the ratio between the two measured quantities, the cross-spectrum and the autospectrum.

It follows from H.1 and H.4 that

$$S_{p_1 p_2} = \frac{S_{AB}}{H_A^* \cdot H_B}$$

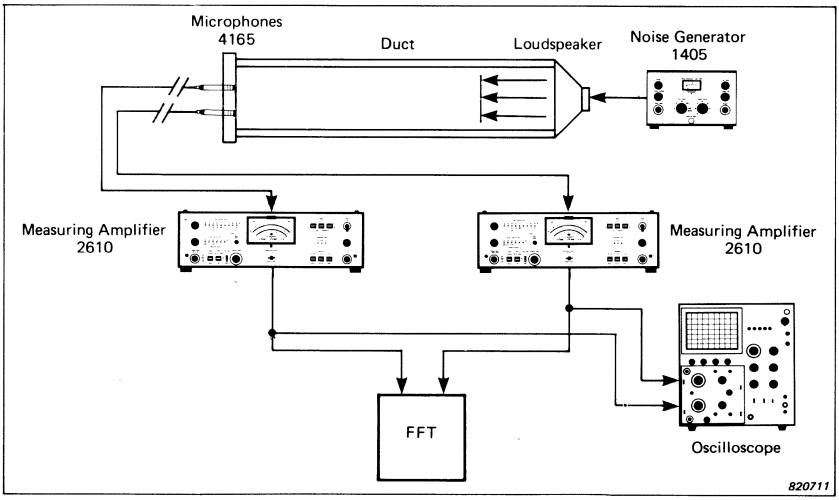

Fig. H1. Microphone calibration in a duct

$$= \frac{S_{AB}}{H_A \cdot H_A^* \cdot H_B/H_A}$$

$$= \frac{S_{AB}}{|H_A|^2 \cdot K_{AB}} \qquad \text{(H.5)}$$

The cross-spectrum S_{AB} between the electrical terminals has to be corrected for the transfer function K_{AB} between the 2 channels and the gain factor $|H_A|^2$ of one of the channels, to obtain the correct cross-spectrum $S_{p_1p_2}$ of the sound field.

H.2 Microphone Switching Method

The measured cross-spectrum is

$$S_{AB} = S_{p_1p_2} \cdot H_A^* \cdot H_B \qquad \text{(H.6)}$$

If the microphone positions are interchanged, see Fig.H2, the measured cross-spectrum is

$$S'_{AB} = S_{p_2p_1} \cdot H_A^* \cdot H_B \qquad \text{(H.7)}$$

or

$$\left(S'_{AB}\right)^* = \left(S_{p_2p_1}\right)^* \cdot H_A \cdot H_B^*$$

$$= S_{p_1p_2} \cdot H_A \cdot H_B^* \qquad \text{(H.8)}$$

combining H.6 and H.8 we obtain

$$S_{p_1p_2} = \sqrt{\frac{S_{AB} \cdot (S'_{AB})^*}{|H_A|^2 \cdot |H_B|^2}} \qquad \text{(H.9)}$$

Selection of the proper root is critical as this determines the indicated direction of the intensity vector. One or more of the following physical assumptions may be invoked:

1. The sound propagates from a known direction.
2. The phase angle of the true cross-spectrum is "small", i.e. it lies between $\pm \pi$.
3. The phase mismatch is small, hence the true cross-spectrum bisects the smaller angle between the two measured cross-spectra.

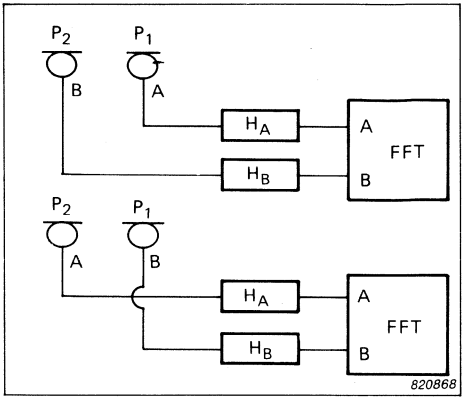

Fig. H2. Interchanging Microphones Procedure

In connection with assumption 2, it should be mentioned that across a node line in a highly reactive field the actual phase angle can be as much as π radians.

H.3 The Modified Microphone Switching Approach

With this method two calibrations are performed, e.g. in the previously mentioned duct. It is *not* assumed that it is exactly the same sound field that is applied to both microphones, only that the sound field is stationary. Thus there is no limitation at high frequencies.

With the first calibration, the measured quantity is (equation H.1. used twice)

$$K_1 = \frac{S_{AB}}{S_{AA}} = \frac{S_{p_1p_2} \cdot H^*_A \cdot H_B}{S_{p_1p_1} \cdot H^*_A \cdot H_A} \qquad \text{(H.10.)}$$

According to this equation it is easy to see that the second calibration with the microphones interchanged gives (see Fig.H2)

$$\frac{S'_{AB}}{S_{BB}} = \frac{S_{p_2p_1} \cdot H^*_A \cdot H_B}{S_{p_1p_1} \cdot H^*_B \cdot H_B} \qquad \text{(H.11)}$$

or

$$K_2 = \frac{(S'_{AB})^*}{S_{BB}} = \frac{S_{p_1p_2} \cdot H^*_B \cdot H_A}{S_{p_1p_1} \cdot H^*_B \cdot H_B} \qquad \text{(H.12)}$$

Combining H.10 and H.12 together, we have

$$\sqrt{K_1/K_2} = H_B/H_A \qquad \text{(H.13)}$$

This quantity inserted in the general equation H.5, instead of K_{AB}, gives

$$S_{p_1p_2} = \frac{S_{AB}}{|H_A|^2 \cdot \sqrt{K_1/K_2}} \qquad \text{(H.14)}$$

Eqn. D.13 (Technical Review No.3 –1982) written in full becomes

$$\hat{I}(r,f) = -\frac{2}{\omega\rho\Delta r} \; Im \; S_{p_1p_2} \qquad \text{(H.15)}$$

APPENDIX I

Digital Time Integrator

Unfortunately an ideal digital integrator does not exist. Due to the importance of the phase response a very simple digital filter given by the equation

$$y_n = x_n + x_{n-1} + y_{n-1} \qquad \text{(I.1)}$$

has been chosen (see Fig.I1).

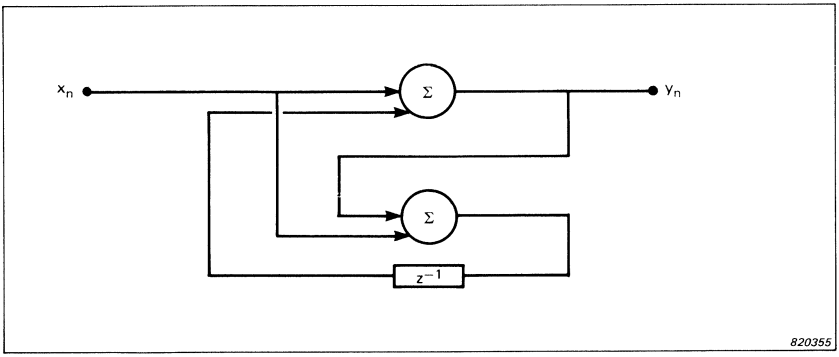

Fig. I1. The digital integrator

A calculation of the amplitude and phase gives

$$|H(\omega)| = |\cot \omega/2f_s|$$

$$\angle H(\omega) = -90° \qquad \text{(I.2)}$$

that is the required phase curve and an amplitude curve which is very easy to correct (see Fig.I2 and I3).

The only consequence of an ideal integrator and that described above, is that if an error signal in one way or another has arisen in the integrator, it will stay there forever, and therefore the integrator has to be cleared before a measurement is started. Note that when the intensity is selected on the 3360, the integrator is cleared automatically.

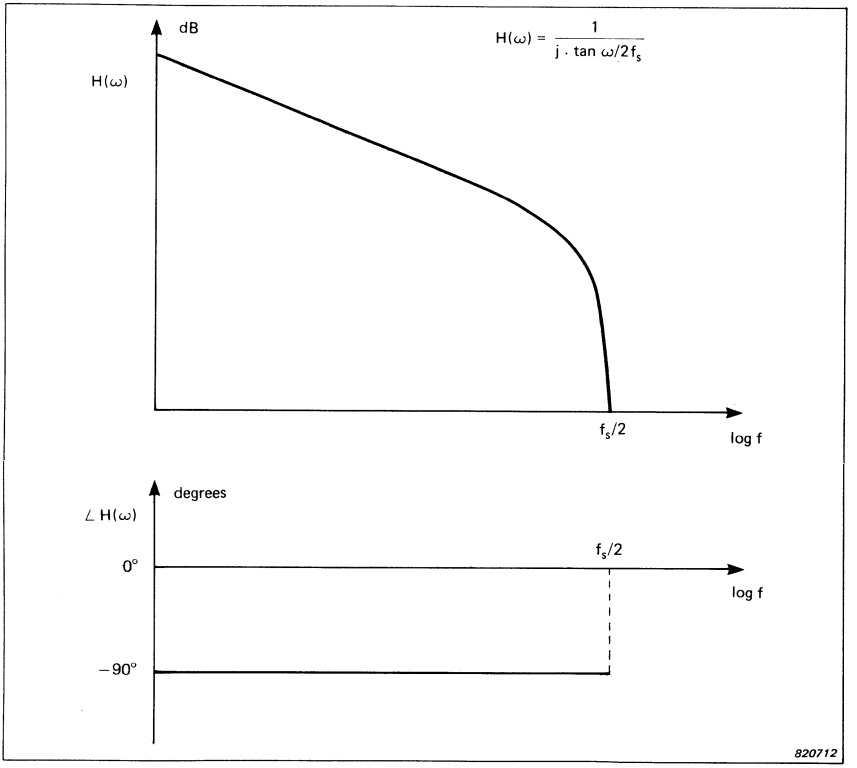

Fig. I2. Amplitude and phase response of the digital integrator

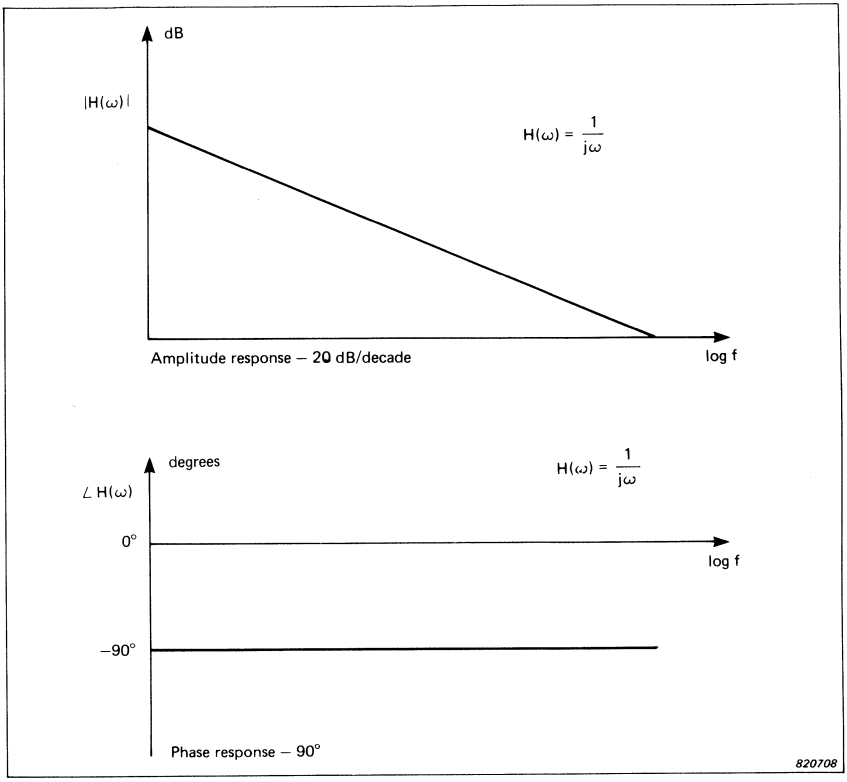

Fig. 13. Amplitude and phase response of an ideal time integrator

FLUTTER COMPENSATION OF TAPE RECORDED SIGNALS FOR NARROW BAND ANALYSIS

by

Jørgen Friis Michaelsen
and
Nis Møller

ABSTRACT

Fluctuations in tape speed of tape recorders cause distortion of recorded and reproduced signals known as flutter. The effect of flutter is seen as noise in the low frequency range below 100 Hz, and as sideband components located around the main data frequency components due to frequency modulation. This article shows how these components are suppressed using a specially developed plug-in module when the tape recorder Type 7005 is used in conjunction with the High Resolution Signal Analyzer Type 2033. Results obtained using this module are also illustrated.

SOMMAIRE

Les variations de la vitesse d'entraînement de la bande sur les enregistreurs magnétiques causent une distorsion des signaux enregistrés et lus connue sous le nom de scintillement. Le scintillement est perçu sous forme de bruit dans la gamme des basses fréquences en dessous de 100 Hz, et sous la forme d'harmoniques situés autour de la composante en fréquence de la donnée principale par suite de la modulation de fréquence. Cet article montre comment ces composantes sont supprimées par un module enfichable spécialement développé pour être utilisé avec l'ensemble de mesure Enregistreur magnétique Type 7005/Analyseur de fréquence haute résolution Type 2033. Les résultats obtenus en utilisant ce module sont également illustrés.

ZUSAMMENFASSUNG

Fluktuationen der Bandgeschwindigkeit bei Magnetbandgeräten rufen Verzerrungen des aufgezeichneten und wiedergegebenen Signals hervor und werden als Gleichlaufschwankungen (Flutter) bezeichnet. Sie zeigen sich als Störsignale im Tieffrequenzbereich unter 100 Hz sowie als durch Frequenzmodulation entstandene Seitenbänder der Hauptfrequenzkomponenten. In diesem Artikel wird gezeigt, wie sich diese Komponenten mit Hilfe eines speziell entwickelten Einschubmoduls unterdrücken lassen, wenn das Meßmagnetbandgerät 7005 in Verbindung mit dem Schmalbandanalysator 2033 eingesetzt wird. Ebenso werden Ergebnisse der Anwendung des Moduls gezeigt.

Introduction

For years instrumentation tape recorders in conjunction with narrow band analyzers have been valuable tools for frequency analysis of signals. Portable, battery driven tape recorders such as the B & K Type 7005, are not only ideal for recording of data in the field, but also for keeping a permanent record of measurements. Measurements can therefore be reproduced whenever desired, thus facilitating analysis of field data to be carried out using sophisticated laboratory based equipment.

However, with the advent of high resolution real time analyzers featuring the zoom technique, the natural weaknesses of the tape drive system of tape recorders have become more evident. Fluctuations in tape speed, result in undesired frequency modulation (flutter) which can distort recorded and reproduced signals. To reduce the effects of this distortion, the B & K tape recorder and systems development groups have produced a special plug-in module which electronically compensates for tape speed variations and thus flutter.

Flutter

One of the limitations that affect performance of tape recorders are the mechanical tolerances of their tape drive system. Very often these cause fluctuations in tape speed, called flutter, which result in unwanted noise modulation of the carrier frequency with FM recording systems.

If a pure sinewave signal is recorded with an FM tape recorder and it is assumed that only one sinusoidal flutter component is present, then the reproduced output after demodulation will be:

$$e_0 = a \cos \omega_f t + \frac{\Delta f_c}{f_c} (1 - a \cos \omega_f t) \sin (\omega_d t - \frac{a\omega_d}{\omega_f} \sin \omega_f t)$$

where a = fractional flutter
$\omega_f = 2\pi f_f$ (f_f is the flutter frequency)
$\omega_d = 2\pi f_d$ (f_d is the data frequency)
f_c = carrier frequency
Δf_c = frequency deviation of carrier

To the original demodulated sine wave $\frac{\Delta f_c}{f_c} \sin \omega_d t$ the flutter of the tape drive system adds three terms:

1) $(a \cos \omega_f t)$ is a noise component due to flutter modulation of the carrier and is independant of the data frequency

2) $(1 - a \cos \omega_f t)$ is the amplitude modulation of the data due to flutter. The influence of this component is usually small and therefore can be neglected.

3) $\frac{a\,\omega_d}{\omega_f} \sin \omega_f t$ represents the frequency modulation of the data due to flutter and results in side-band components located on either side of the main data frequency component. These are separated by f_f and have magnitudes derived from Bessel functions of $\Delta f_f / f_c$.

The effect of the above components on the frequency spectrum of reproduced data may be represented schematically as shown in Fig. 1. In the following the effects of the noise and frequency modulation

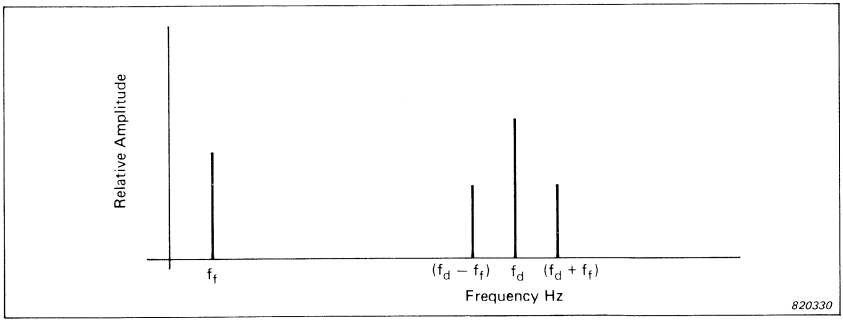

Fig. 1. Frequency spectrum of the demodulated output of an FM tape recorder showing the influence of flutter

components (1) and (3) will be considered. In addition, suitable compensating techniques for suppressing unwanted interference caused by these components will be discussed.

Practical Influence of Flutter

As an example of the influence of flutter on frequency analyses, measurements were carried out on a B & K Instrumentation Tape Recorder Type 7005. With this recorder the inherent flutter weighted in accordance with DIN 45 507, is less than 0,06%, which is typical, if not better than most commercially available portable instrumentation tape recorders. This is borne out by the narrow-band analysis shown in Fig. 2 which was measured using the B & K High Resolution Signal Analyzer Type 2033.

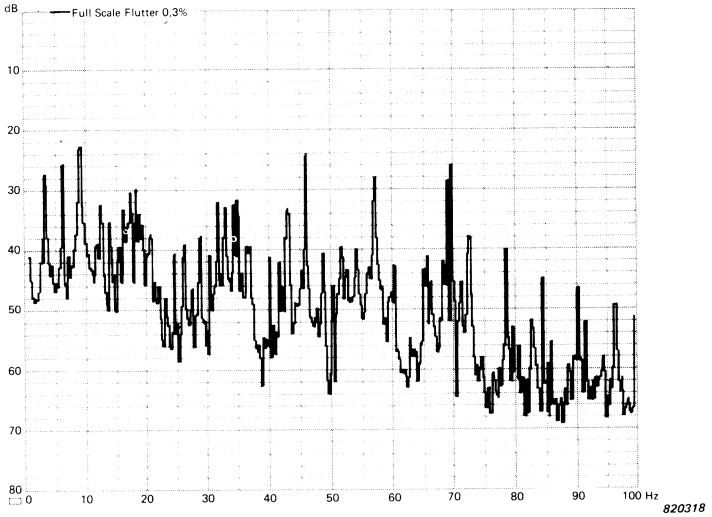

Fig. 2. Narrow band analysis of FM record-reproduce noise produced by Tape Recorder Type 7005 showing influence of flutter

The modulation noise caused by the inherent flutter of the 7005 can be seen by comparing Figs. 3 and 4. Fig. 3 shows the narrow band frequency spectrum of a 1 kHz sine wave reproduced by one of the FM Channels of the Recorder with its FM Modulator and Demodulator directly interconnected (i.e. bypasses the recording tape and tape drive system of the recorder), while Fig. 4 shows the same signal but when recorded and reproduced via tape. To obtain a more detailed view of

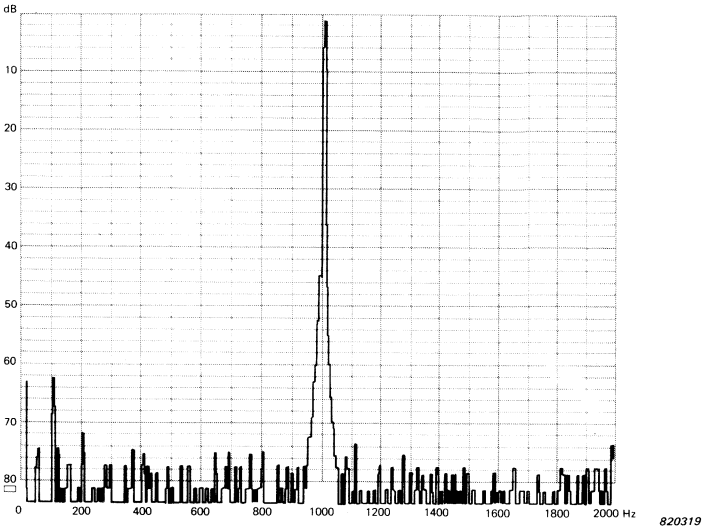

Fig. 3. Narrow band analysis of 1 kHz sine wave reproduced via one of the FM channels of a Tape Recorder Type 7005, but bypassing the tape drive and recording tape.

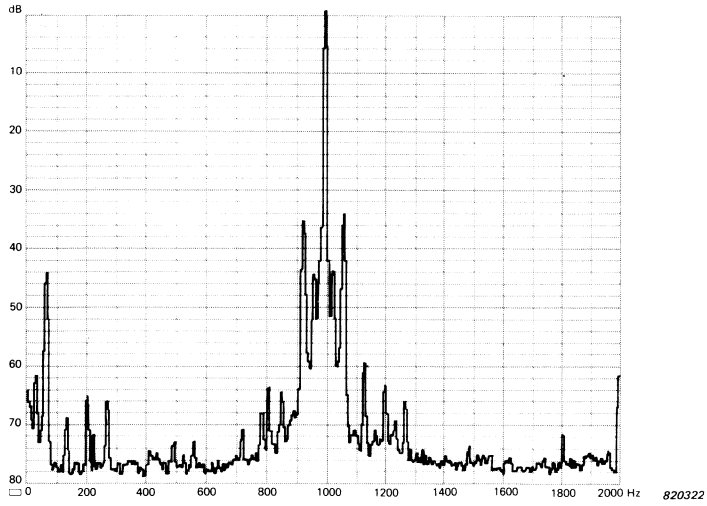

Fig. 4. Narrow band analysis of on-tape 1 kHz sine wave showing influence of FM record-reproduce flutter with Tape Recorder Type 7005

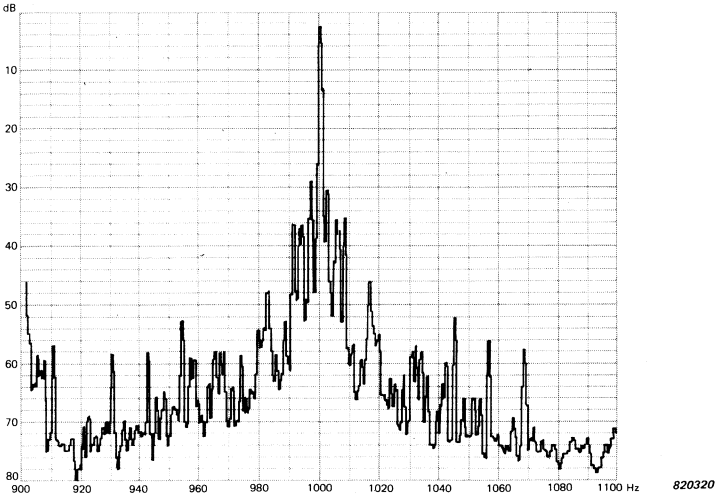

Fig. 5. Expanded narrow band analysis of on-tape 1 kHz sine wave showing influence of FM record-reproduce flutter with Tape Recorder Type 7005

the side band components around 1 kHz, a × 10 Zoom capability of the 2033 Analyzer can be used. A typical spectrum obtained with such a zoom for a 1 kHz sinusoidal signal is shown in Fig. 5.

From the above it can be seen that even with tape recorders of the very best quality, flutter can limit the resolution obtained with narrow band analyses, particularly where investigation of low level signal components is involved.

Flutter Compensation

In order to limit the effects of record-reproduce flutter, several means of electrical compensation are available. The first of these is to record a fixed frequency reference carrier of 54 kHz (for use with tape speed of 381 cms/s)on tape via a separate channel, which on playback can be demodulated and subtracted from the reproduced data. It is this method which is provided with the 7005 and is useful for suppressing the flutter noise component a cos $\omega_f t$ (i.e. f_f in Fig. 1, noise component *not* related to data frequency) previously specified. With flutter components produced by external movement and vibration of the recorder, as much as 30 dB of suppression can be obtained. However, where inherent flutter is concerned, the maximum suppression is normally not as great. Compare Figs.4 and 6 for frequency components below 100 Hz.

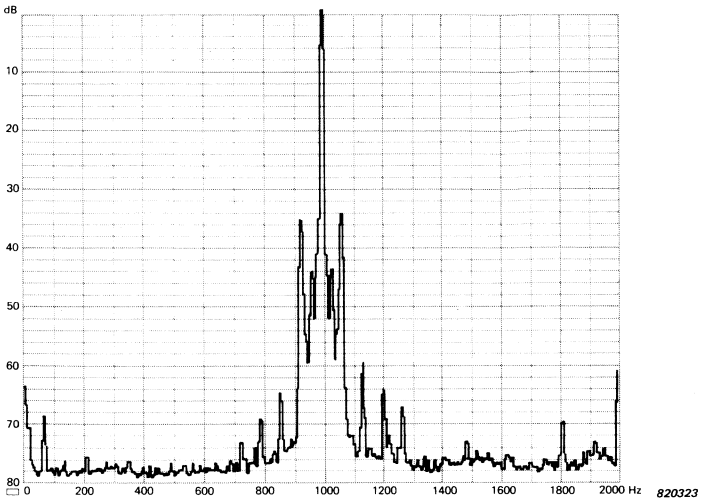

Fig. 6. Narrow band analysis of on-tape 1 kHz sine wave reproduced with FM Flutter Compensation selected on Tape Recorder Type 7005.

Another means of flutter compensation is available using the external sampling facility of the High Resolution Signal Analyzer Type 2033. For this purpose a special Sampling Frequency Module WB 0722 has been developed. This plugs into one of the channels of the 7005 and is used for recording an accurate 51,2 kHz (at tape speed of 381 cms/s) reference frequency on tape, which on playback to the 2033 facilitates sampling at a constant rate per tape length. Fig. 7 shows the principle of the set-up used.

The 51,2 kHz reference corresponds to the sampling frequency of the highest frequency range (0 to 20 kHz) of the 2033. For correct sampling with the other frequency range settings of the 2033, corresponding settings may be selected on WB 0722 which divide the frequency of the reproduced reference accordingly.

Often data containing low frequency signals, are recorded at 38,1 cms/s and played back at 381 cms/s. In this case a reference frequency of 5,12 kHz is recorded on tape which is automatically transformed to 51,2 kHz on playback at 381 cms/s.

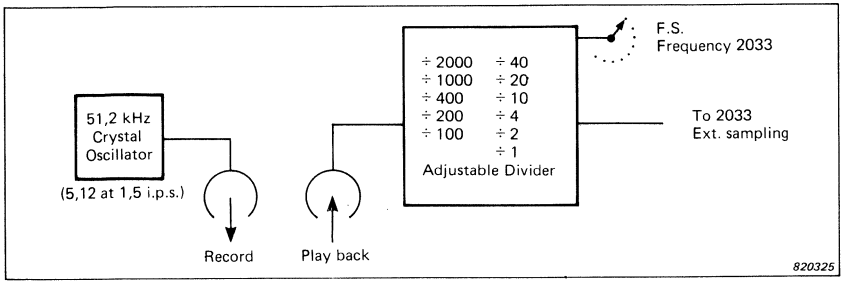

Fig. 7. Use of Sampling Frequency Module WB 0722 with Tape Recorder Type 7005 to facilitate flutter compensation with aid of the external sampling facility of Signal Analyzer Type 2033

A narrow band analysis obtained using the above method of sampling frequency flutter compensation, is shown in Fig. 8. Comparison with Fig. 4 shows that it is capable of providing as much as 20 dB suppression of unwanted side-band components produced by flutter, thus enabling very low amplitude signal components to be accurately analyzed.

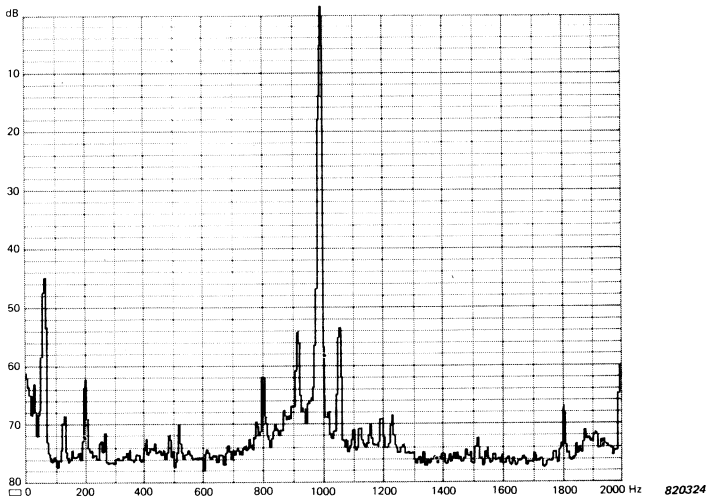

Fig. 8. Narrow band analysis of on-tape 1 kHz sine wave using the external sampling facility of Signal Analyzer Type 2033 for flutter compensation

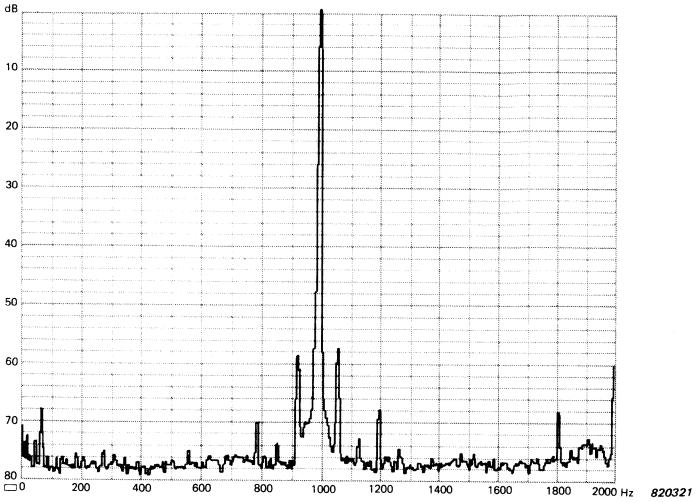

Fig. 9. Narrow band analysis of on-tape 1 kHz sine wave with FM flutter compensation by Tape Recorder Type 7005 plus the sampling facility of Signal Analyzer Type 2033

In Fig. 9 is shown a narrow band analysis obtained using both the above methods of flutter compensation simultaneously. To save recording two separate references only the sampling frequency reference need be recorded for operating the flutter compensation and external sampling facilities of the Recorder and Signal Analyzer. For this purpose the Sampling Frequency Module WB 0722 should be employed with channel 2 of the 7005. A minor disadvantage is that reproduced data will be offset by a small DC voltage owing to sampling frequency not being identical with the carrier frequency used for recording.

To conclude it can be seen that the above techniques provide a significant reduction in broadband noise and modulation noise with tape recorded data, thus greatly expanding the uses of Tape Recorder Type 7005 in the field of high resolution, narrow band frequency analysis.

Reference

[1] PEAR, C.B.Jr. Magnetic Tape Recording in Science and Industry

News from the Factory

Digital Stroboscope Type 4913 and Fibre-Optic Source Type 4915

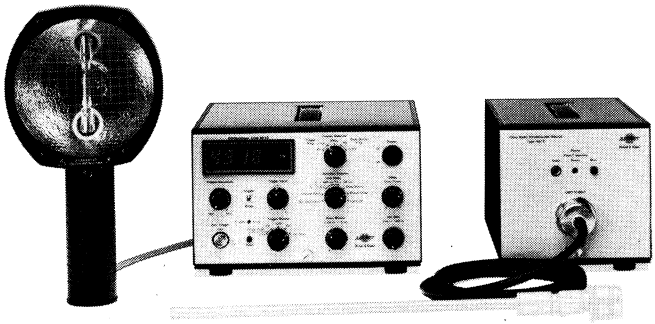

The Digital Stroboscope Type 4913 is a stroboscopic motion analyzer/ tachometer and includes a built-in digital display for accuracy and versatility. Using its high intensity, hand-held flash source, a stationary or slow moving image of all kinds of rapid repetitive motion can be obtained, making it extremely easy to observe the precise behaviour of vibration test components, engines, machines etc. whilst actually in motion.

The 4913 may be synchronized with motion frequencies as high as 10 kHz (600 k r/min) and can be triggered from an internal generator, power line or external source such as a contact-free tachometer probe. Separate modes with adjustable time and phase delay permit precise measurement and observation at any required point in the motion cycle and a "Slow Motion" mode enables objects to be viewed with an apparent motion frequency of 0,05 to 5 Hz.

Using the 4-digit display of the 4913 direct reading of motion frequency or speed, time or phase delay is possible which is extremely useful for measurements and setting-up of the instrument. Additional features are choice of local or remote control, plus single flash operation for photographic purposes.

As an optional light source Type 4913 can be coupled with the Fibre-Optic Stroboscope Source Type 4915. Light transmission is via a resilient 1,8 m long fibre-optic cable AE 6000 which outputs a convenient point source of illumination that is ideal for examination of small mechanical components, intricate mechanisms and microscopic specimens etc. Furthermore a matching Endoscope Probe can be fitted, whereby internal surfaces, bearings and working mechanisms actually hidden inside engines and machines can be inspected. Suitable probes are available from the West German Companies Richard Wolf GmbH and Karl Storz GmbH.

Precision Integrating Sound Level Meters Types 2221 and 2222

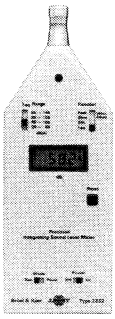

The Type 2221 and Type 2222 are Precison Integrating Sound Level Meters of pocket size complying with Proposed IEC Standard for Precision Integrating Sound Level Meters Type 1P and IEC 651 Type 1, DIN-IEC 651 Class 1, BS 5969 Type 1, ANSI S1.4.1971 Type 1 and its proposed revision. They offer four basic measurements: L_{eq}, SEL, Max Hold Peak (with linear weighting) and Max Hold "Fast" for Type 2221 or Max Hold "Slow" for Type 2222. The measurement range is displayed in four overlapping sub-ranges giving a measurement span from 25 dB to 145 dB for L_{eq} measurements.

A microprocessor ensures the calculation of true L_{eq} or SEL values at intervals of 0,5 s, and the user is able to switch between the two calculations during measurement, the results being directly displayed with a resolution of 0,1 dB. A Pause switch permits spatial integration of sound pressure level.

The large digital display makes reading errors virtually impossible. In addition to the $3^1/_2$ digits, the display indicates six other symbols: overload, under range, battery state, time exceeded (L_{eq} measurements) and A or linear weightings. An AC Output allows recordings on tape or paper.

The Types 2221 and 2222 are used for assessment of fluctuating or cyclical noises (L_{eq}), and for assessment of single noise events (SEL) or max levels (Max Hold).